Identification of the Parameters of the Beeler–Reuter Ionic Equation With a Partially Perturbed Particle Swarm Optimization

Fulong Chen, Angdi Chu, Xuefei Yang, Yao Lei, and Jizheng Chu*

***Abstract*—A partially perturbed particle swarm optimization (PPSO) has been proposed for identifying the parameters of the Beeler–Reuter (BR) equation from action potential data. In the PPSO algorithm, the 63 BR equation parameters are divided into groups, and parameter patterns are made from the combination of the groups. PPSO enhances the capability of conventional particle swarm optimization (CPSO) by partially perturbing the coordinates of the globally best particle with the patterns when the searching process is locally confined. "Experimental data" were produced for cardiac myocytes simulated by the BR equation and the equation of Luo and Rudy (1991), and were used to test the algorithm of PPSO. The test results show that PPSO was able to identify the parameters of the BR equation effectively for different cardiac myocytes, while still retaining the conceptual simplicity and easy implementation of CPSO.**

***Index Terms*—Beeler–Reuter (BR) equation, cardiac myocyte, parameter identification, particle swarm optimization (PSO).**

I. Introduction

DYNAMIC mathematical models have been successfully used to describe the electrical activities of cardiac myocytes and have served as an important measure for understanding the molecular mechanism of normal and abnormal heart behaviors. Most of the existing electrophysiological models for cardiac myocytes stem from the conductance-based compartment model established by Hodgkin and Huxley [1], and the famous ones among them include: 1) the modified Hodgkin–Huxley equations of Noble [2] for the action potential and pacemaker potential of Purkinje fibers; 2) the McAllister-Noble-Tsien (MNT) model for reconstructing the electrical activities of Purkinje fibers developed by McAllister *et al.* [3]; 3) the BR ionic equation of Beeler and Reuter [4], which has a calcium channel to reconstruct the action potential of ventricular myocardial fibers; and 4) modifications to the McAllister-Noble-Tsien (MNT) model and BR equation proposed by Drouhard and Roberge [5], [6]. With the advance of technology for measuring electrical activities of myocytes, more delicate models such as the one of DiFrancesco and Noble [7], are expected to account for more details of cardiac activities with more parameters and higher complexity.

The Hodgkin–Huxley type expressions for cardiac myocytes are highly nonlinear. The identification of parameters of such a model often constitutes an optimization problem of multiple dimensions and numerous local minima. For such problems, nonclassical searching methods with some degree of randomness are necessary, and recently several authors have made their contributions: Dokos and Lovell [8] estimated the BR equation parameters with a gradient-based curvilinear search algorithm, Syed et al. [9] fit the atrial cell action potential parameters using genetic algorithms, and Liu et al. [10] employed a modified Nelder–Mead search combined with the particle swarm optimization (PSO) to evaluate the parameters of the Bueno–Orovio phenomenological model. Identification of electrophysiological models is computationally intensive. Mathavan [11] reported that several days were needed to indentify a component current model of 26 parameters using the curvilinear search algorithm [8].

This paper is aimed at identification of the parameters of the BR equation for its importance in electrophysiology with PSO for its conceptual simplicity and easy implementation. As demonstrated by Dokos and Lovell [8], estimating the 63 BR equation parameters is a difficult problem that is high dimensional and ill conditioned in the sense that derivatives of the membrane voltage with respect to different parameters are disparate by about eight orders of magnitude. For this problem, multiple local minima exist and the optimal solution is not unique. Our experience showed that the conventional particle swarm optimization (CPSO) as first proposed by Kennedy and Eberhart [12] would soon and easily fail in searching the BR equation parameters. Further observations indicated that in the searching process of CPSO, some parameters reached positions very close to the desired values at some instants and went away at other instants. This observation gives us a clue for building heuristic strategies with which a nonclassical searching method may work more efficiently.

II. Beeler–Reuter (BR) Ionic Equation

The BR ionic equation [4], [8] expresses the transmembrane potential (V_m, mV) of a cardiac myocyte as

Manuscript received June 1, 2012; revised July 31, 2012; accepted August 24, 2012. Date of publication August 31, 2012; date of current version November 22, 2012. *Asterisk indicates corresponding author.*

F. Chen, X. Yang, and Y. Lei are with the College of Information Science and Technology, Beijing University of Chemical Technology, Beijing 100029, China (e-mail: 2010000764@grad.buct.edu.cn; 2011200822@grad.buct.edu.cn; 2009000764@grad.buct.edu.cn).

A. Chu is with the School of Life Science and Technology, Huazhong University of Science and Technology, Wuhan 430074, China (e-mail: chuangdi@163.com).

*J. Chu is with the College of Information Science and Technology, Beijing University of Chemical Technology, Beijing 100029, China (e-mail: chujz@mail.buct.edu.cn).

Color versions of one or more of the figures in this paper are available online at http://ieeexplore.ieee.org.

Digital Object Identifier 10.1109/TBME.2012.2216265

0018-9294/$31.00 © 2012 IEEE

TABLE I
PARAMETERS FOR CALCULATING COEFFICIENTS α_y AND β_y OF THE GATING VARIABLE EQUATIONS

	α_{x1}	β_{x1}	α_m	β_m	α_h	β_h	α_j	β_j	α_d	β_d	α_f	β_f
C_1	p_{23}	p_{27}	0	p_{34}	p_{36}	p_{38}	p_{41}	p_{45}	p_{48}	p_{52}	p_{56}	p_{60}
C_2	p_{24}	p_{28}	0	p_{35}	p_{37}	0	p_{42}	0	p_{49}	p_{53}	p_{57}	p_{61}
C_3	0	0	p_{31}	0	0	0	0	0	0	0	0	0
C_4	0	0	p_{32}	0	0	0	0	0	0	0	0	0
C_5	p_{25}	p_{29}	p_{33}	0	0	p_{39}	p_{43}	p_{46}	p_{50}	p_{54}	p_{58}	p_{62}
C_6	p_{26}	p_{30}	-1	0	0	p_{40}	p_{44}	p_{47}	p_{51}	p_{55}	p_{59}	p_{63}

$$\frac{dV_m}{dt} = -\left(\frac{1}{C_m}\right)(i_{k1} + i_{x1} + i_{\mathrm{Na}} + i_s - i_{\mathrm{stim}}) \tag{1}$$

where $C_m = 1$ μF/cm^2 is the membrane capacitance, i_{k1} the time-dependent outward potassium current, i_{x1} the time-activated outward current, i_{Na} the inward sodium current, i_s the slow inward current carried mainly by calcium ions, and i_{stim} the external stimulus current, with all the currents being in μA/cm^2. The ionic currents are calculated, respectively, as:

$$i_{k1} = \frac{p_1\{\exp[p_2(V_m + p_3)] - 1\}}{\exp[p_4(V_m + p_5)] + \exp[p_6(V_m + p_5)]} + \frac{p_7(V_m + p_8)}{1 - \exp[p_9(V_m + p_8)]} \tag{2}$$

$$i_{x1} = \frac{x_1 p_{10}\{\exp[p_{11}(V_m + p_{12})] - 1\}}{\exp[p_{13} V_m]} \tag{3}$$

$$i_{\mathrm{Na}} = (p_{14} m^3 hj + p_{15})(V_m - p_{16}) \tag{4}$$

$$i_s = p_{17} df(V_m - p_{18} - p_{19}\ln[\mathrm{Ca}]_i) \tag{5}$$

where $[\mathrm{Ca}]_i$ is the intracellular Ca^{2+} concentration in M determined by the following conservation equation:

$$\frac{d[\mathrm{Ca}]_i}{dt} = p_{20} i_s + p_{21}(p_{22} - [\mathrm{Ca}]_i) \tag{6}$$

and $y = x_1, m, h, j, d,$ and f are the dimensionless gating variables described by

$$\frac{dy}{dt} = \alpha_y(1 - y) - \beta_y y \tag{7}$$

with α_y and β_y being the rate coefficients in ms^{-1} correlated with the potential by the following equation:

$$\alpha_y, \beta_y = \frac{C_1 \exp(C_2 V_m) + C_3(V_m + C_4)}{\exp[C_5(V_m + C_4)] + C_6} \tag{8}$$

where $C_1 - C_6$ are parameters related to each gating variable as shown in Table I.

From the aforementioned description, we know that the BR equation consists of eight ordinary differential equations (ODEs) in (1), (6), and (7) with 63 parameters $P = \{p_i, i = 1, 2, \ldots, 63\}$. Table II lists a set of values for the parameters, the default parameters hereafter and denoted by $\bar{P} = \{\bar{p}_i, i = 1, 2, \ldots, 63\}$, given by Dokos and Lovell [8].

In solving the eight ODEs of the BR equation with function ode15 s of MATLAB R2009 a (MathWorks, Inc., 2009), it may be helpful to note the following two points.

1) Determination of the resting potential, currents, and calcium concentration. Each set of values for the 63 BR equation parameters corresponds to certain resting potential, currents, and calcium concentration, which are the initial values of the eight ODEs and can be computed before the ODEs are solved. The eight algebraic equations from zeroing the time derivatives of the eight ODEs determine the resting values of the potential, currents, and calcium concentration. Since the six gating variables can be expressed as a function of V_m

$$y = \frac{\alpha_y}{\alpha_y + \beta_y} \tag{9}$$

only the resting V_m and $[\mathrm{Ca}]_i$ are to be found from the following two simultaneous equations:

$$i_{k1} + i_{x1} + i_{\mathrm{Na}} + i_s = 0 \tag{10}$$

$$p_{20} i_s + p_{21}(p_{22} - [\mathrm{Ca}]_i) = 0 \tag{11}$$

which can be solved efficiently with a nested secant method with V_m and $[\mathrm{Ca}]_i$ being the iterating variables of the outer and inner loops, respectively.

2) Acceleration for solving the BR equation. It is observed that the eight ODEs behave mildly except in a duration of about 10 ms starting from the injection of a stimulus current where they exhibit considerable stiffness. Therefore, the solution time can be greatly reduced by setting a large value (1 ms in this study) for the maximum time step (MaxStep) of ODE15 s. To guarantee the solution precision, we set the relative error tolerance of ODE15 s to be small (10^{-5} in this study). Linear interpolation was then employed to sample the membrane potential, currents, and calcium concentration at desired time instants.

TABLE II
DEFAULT VALUES FOR THE 63 BR EQUATION PARAMETERS

i	$\bar{p}_i$	i	$\bar{p}_i$	i	$\bar{p}_i$
1	1.4000	22	1.0000×10^{-7}	43	-0.2000
2	0.0400	23	0.0018	44	$5.9565\times10^{+6}$
3	85.0000	24	0.0830	45	7.3598
4	0.0800	25	0.0570	46	-0.1000
5	53.0000	26	0.0578	47	24.5325
6	0.0400	27	8.7142×10^{-4}	48	0.0697
7	0.0700	28	-0.0600	49	-0.0100
8	23.0000	29	-0.0400	50	-0.0720
9	-0.0400	30	2.2255	51	0.6977
10	0.1973	31	-1.0000	52	0.0037
11	0.0400	32	47.0000	53	-0.0170
12	77.0000	33	-0.1000	54	0.0500
13	0.0400	34	0.7096	55	0.1108
14	4.0000	35	-0.0560	56	1.4383×10^{-4}
15	0.0030	36	5.4980×10^{-10}	57	-0.0080
16	50.0000	37	-0.2500	58	0.1500
17	0.0900	38	10.7578	59	0.0150
18	-82.3000	39	-0.0820	60	1.4391
19	-13.0287	40	6.3281	61	-0.0200
20	-1.0000×10^{-7}	41	0.0011	62	-0.2000
21	0.0700	42	-0.2500	63	403.4300

III. Problem of Identifying the BR Equation Parameters

Parameter identification can be generally formulated as a problem of minimization:

$$\min_X g(X) \tag{12}$$

where $X \in \mathrm{R}^m$ is the vector of the parameters scaled to be $0 \leq X(i) \leq 1$ for $i = 1, 2, \ldots, m$, and g:$\mathrm{R}^m \rightarrow \mathrm{R}^1$the fitness.

For identifying the BR equation parameters, $m = 63$ and

$$p_i = p_{\min,i} + X(i)\left(p_{\max,i} - p_{\min,i}\right) \tag{13}$$

where $p_{\min,i}$ and $p_{\max,i}$ are the lower and upper bounds for parameter p_i. For later use, let $P_{\min} = \{p_{\min,i}, i = 1, 2, \ldots, 63\}$ and $P_{\max} = \{p_{\max,i}, i = 1, 2, \ldots, 63\}$. The fitness is defined as

$$g = \sqrt{\frac{1}{K}\sum_{k=1}^{K}\left(\frac{\bar{V}_{m,k} - V_{m,k}}{\bar{V}_{\max,m} - \bar{V}_{\min,m}}\right)^2} \tag{14}$$

where k is the index number of the datum sampled at instant t_k in ms, K the total number of sampled data, $V_{m,k}$ and $\bar{V}_{m,k}$ are, respectively, the transmembrane potentials at t_k calculated by the BR equation and measured experimentally, and $\bar{V}_{\max,m}$ and $\bar{V}_{\min,m}$, respectively, the maximum and minimum of the measured potential.

IV. Partially Perturbed Particle Swarm Optimization (PPSO)

As one of the swarm intelligence algorithms, the PSO has received much attention for its conceptual simplicity and easy implementation ever since its birth in 1995 [12]. Numerous efforts have been witnessed in its application and improvement. As a matter of fact, PSO has become an idea common to a huge number of optimization algorithms. For statement convenience, we term the algorithm introduced in this section as the CPSO.

In CPSO, we have particles in the searching space of a minimization problem. The coordinates of a particle represent a candidate solution, and the objective function at a candidate solution is called the fitness of the corresponding particle. The particles fly in the searching space in a manner designed to achieve a better fitness, which constitutes the searching procedure. The flying process of particles from the positions at one time instant to the positions at next time instant is called evolution, and a particle therefore has its own history of evolution designated by generation.

For the problem in (12), CPSO renews the position of particle τ ($\tau = 1, 2, \ldots, n$) by

$$X_\tau^{(l)} = X_\tau^{(l-1)} + u_\tau^{(l)} \tag{15}$$

where superscript l is the number of the evolving generation and u a vector of the flying speed computed as

$$u_\tau^{(l)} = \omega u_\tau^{(l-1)} + c_1 R_1\left[L_\tau^{(l-1)} - X_\tau^{(l-1)}\right] + c_2 R_2\left[G^{(l-1)} - X_\tau^{(l-1)}\right] \tag{16}$$

where $L_\tau^{(l)}$ is the best position (with lowest fitness value) ever achieved by particle τ, $G^{(l)}$ the best position ever achieved by all the n particles, ω the inertia weight, c_1 and c_2 are the acceleration constants, and R_1 and R_2 two random numbers generated independently from a uniform distribution over [0, 1] for each particle at each generation.

To increase the heuristics of the aforementioned algorithm, the inertia weight is adapted in this study as suggested by Yang *et al.* [13]:

$$\omega = \exp\left[-\alpha^{(l-1)}\Big/\alpha^{(l-2)}\right] \tag{17}$$

where

$$\alpha^{(l)} = \frac{1}{n}\sum_{\tau=1}^{n}\left|g(X_\tau^{(l)}) - g(G^{(l)})\right|. \tag{18}$$

Our experience showed that in identifying the BR equation parameters, the CPSO was always confined to a local minimum at early generations of its evolution. In fact, this difficulty is not peculiar to the task of this study, and generally exists in multidimensional problems with complex dependence among variables and parameters. Though the global optimum is theoretically ensured by the evolution strategy of CPSO, the high dimensions and complexities of real problems often make such a searching unrealistic.

It was observed that at a minimum to which CPSO was confined, some of the parameters were at or close to their "true values," but others were far from their "true values." If we have a heuristic rule to improve the "lost" parameters only, CPSO will get rid of the confinement of a local minimum. Such a rule can be realized by perturbing the parameters by groups. For the problem in (12), the m parameters can be divided into N_g groups according to some grouping scheme, and these groups are combined to produce $N = \sum_{k=1}^{N_g} C_{N_g}^k$ parameter patterns:

$$E_\lambda = \{e_{\lambda,i}\,|_{i=1,2,\ldots,m}\}, \quad \lambda = 1, 2, \ldots, N \tag{19}$$

where $e_{\lambda,i} = 1$ if p_i is included in pattern λ or 0 if not.

Based on the parameter patterns, CPSO in the above section is modified to form the following stepwise procedure for our PPSO:

Step 1: Give the number of particles n, acceleration constants c_1 and c_2, number of the parameter patterns N, parameter patterns $E_\lambda, \lambda = 1, 2, \ldots, N$, tolerable number of consecutive generations of nonimprovement $q_{\max}$, maximum number of generations $l_{\max}$, and minimum fitness $g_{\min}$.

Step 2: Initialize the inertia weight $\omega = 0.6$, number of the current generation $l = 0$, number of consecutive generations of nonimprovement $q = 0$, and the positions and velocities of the n particles. For particle τ

$$X_\tau^{(0)}(i) = R_{\tau,i}, u_\tau^{(0)}(i) = 0.1\ R'_{\tau,i} \tag{20}$$

where $R_{\tau,i}$ and $R'_{\tau,i}$ are random numbers generated independently from a uniform distribution in [0, 1] for each dimension of each particle.

Step 3: Compute the fitness for all the particles: $g_\tau^{(l)}, \tau = 1, 2, \ldots, n$. If $l \equiv 0$, initialize the best position and fitness ever

achieved by each particle

$$L_\tau^{(l)} = X_\tau^{(l)}, U_\tau^{(l)} = g_\tau^{(l)}. \tag{21}$$

Then, find the best particle (σ) in the current generation

$$g_\sigma^{(l)} = \min\left\{g_\tau^{(l)}, \tau = 1, 2, \ldots, n\right\} \tag{22}$$

and record the best position and fitness ever achieved by all the particles

$$G^{(l)} = X_\sigma^{(l)}, U^{(l)} = g_\sigma^{(l)}. \tag{23}$$

If $l > 0$, the best position $L_\tau^{(l)}$ and fitness $U_\tau^{(l)}$ ever achieved by each particle are first recorded: if $U_\tau^{(l-1)} > g_\tau^{(l)}$, renew them according to (21); otherwise, keep them unchanged

$$L_\tau^{(l)} = L_\tau^{(l-1)}, U_\tau^{(l)} = U_\tau^{(l-1)}. \tag{24}$$

Then, find the best particle (σ) in the current generation with (22). Renew the best position$G^{(l)}$and fitness$U^{(l)}$ever achieved by all the particles according to (23) and set the number of consecutive generations of nonimprovement $q = 0$ if $U^{(l-1)} > g_\sigma^{(l)}$; otherwise, keep them unchanged:

$$G^{(l)} = G^{(l-1)}, \quad U^{(l)} = U^{(l-1)} \tag{25}$$

and increase q by 1.

Step 4: If the fitness value is good enough $(g < g_{\min})$ or $l \geq l_{\max}$ or $q > 5q_{\max}$, output $G^{(l)}$ and $U^{(l)}$, stop; otherwise, go to the next step.

Step 5: If $q < q_{\max}$, go to Step 6; else, PPSO is confined to a local minimum and the following two substeps are executed.

Step 5.1: With the N patterns, generate N particles by perturbing the globally best particle:

$$\tilde{X}_\lambda(i) = \begin{cases} \left(1 + \dfrac{R_\lambda - 0.5}{40}\right) G^{(l)}(i), & (\text{if } e_{\lambda,i} \equiv 1) \\ G^{(l)}(i), & (\text{otherwise}) \end{cases} \tag{26}$$

for $\lambda = 1, 2, \ldots, N$ and $i = 1, 2, \ldots, m$, while noting the constraint of $0 \leq \tilde{X}_\lambda(i) \leq 1$. In the above equation, R_λ is a random number generated independently from a uniform distribution in [0, 1] for each particle.

Step 5.2: Calculate the fitness $(\tilde{g}_\lambda)$ for each of the above N particles, and find the best one (σ) among them

$$\tilde{g}_\sigma = \min\left\{\tilde{g}_\lambda, \lambda = 1, 2, \ldots, N\right\}. \tag{27}$$

If $U^{(l)} > \tilde{g}_\sigma$, renew the best position $G^{(l)}$ and fitness $U^{(l)}$ ever achieved by all the particles

$$G^{(l)} = \tilde{X}_\sigma, \quad U^{(l)} = \tilde{g}_\sigma \tag{28}$$

and the worst particle r $(U_r^{(l)} > U_\tau^{(l)}$ for $\tau = 1,2, \ldots, n, \tau \neq r)$

$$L_r^{(l)} = \tilde{X}_\sigma, \quad U_r^{(l)} = \tilde{g}_\sigma \tag{29}$$

and set $q = 0$; otherwise, let $q = q + 1$. Go to Step 6.

Step 6: If $l \geq 2$, adapt the inertia weight ω according to (17). Renew the velocities of all the particles according to (16), and then the positions according to (15) while noting the lower and upper bounds (0−1) for X: $X\ (i) = 0$ if $X(i) < 0$, and $X(i) = 1$ if $X(i) > 1$, for $i = 1, 2, \ldots, m$, let $l = l + 1$ and go back to Step 3.

TABLE III
GROUPS OF THE PARAMETERS OF THE BR MODEL

group	the BR equation parameters		
	scheme 1	scheme 2	scheme 3
1	$p_{1\text{-}9}$	$p_{1\text{-}20}$	$p_{2\text{-}5,7,9,11,12,17\text{-}19,60,63}$
2	$p_{10\text{-}13,23\text{-}30}$	$p_{21\text{-}40}$	$p_{1,8,10,13,20,21,23\text{-}25,32,33,35,48,50,52\text{-}54}$
3	$p_{14\text{-}16,31\text{-}47}$	$p_{41\text{-}63}$	$p_{6,14\text{-}16,28,31,34,38\text{-}40,42,43,46,51,55,56,58,59,61,62}$
4	$p_{17\text{-}12,48\text{-}63}$	-	$p_{26,27,29,30,37,45,47,49,57}$
5	-	-	$p_{22,41}$
6	-	-	$p_{36,44}$

TABLE IV
FIFTEEN PATTERNS OF PARAMETERS TO BE PERTURBED FOR SCHEME 1

pattern	group(s)	pattern	groups	pattern	groups
1	1	6	1,3	11	1,2,3
2	2	7	1,4	12	1,2,4
3	3	8	2,3	13	1,3,4
4	4	9	2,4	14	2,3,4
5	1,2	10	3,4	15	1,2,3,4

In applying the aforementioned algorithm (PPSO) to identify the BR equation parameters in the next section, three grouping schemes were used and the corresponding parameter groups are listed in Table III. In scheme 1, the 63 parameters are divided into four groups according to the four BR membrane currents models in (2) – (5) to which the parameters are, respectively, attributed. Scheme 2 divides the parameters into three simple groups quite arbitrarily. Scheme 3 classifies the parameters into six groups according to their sensitivities, and the derivatives of transmembrane voltage with respect to the parameters at the default $(\bar{P})$ in groups 1–6 range, respectively, over [10 078, 851.78], [529.51, 42.292], [29.917, 2.5058], [1.5014, 0.18021], [0.02317, 0.01285], and [0.00528, 0.00061]. The 15 patterns of parameters to be perturbed are listed in Table IV for grouping scheme 1. In addition, two points should also be noted:

1) For a PSO-type algorithm such as PPSO described above, more particles obviously bring a better coverage of the searching space in each generation of its evolution, but more time is consumed. A stochastic optimization problem could be formulated to determine the best number of particles for a specific problem with given computing resources. In this paper, however, n was roughly chosen by preliminary calculations.
2) Not every particle produced by (20) at the initialization step or renewed by (15) or (26) is a set of feasible parameters for the BR equation. It is necessary for a feasible set of BR equation parameters to have certain resting state which can be found by the method in Section II. In Step 2, an initial particle should be regenerated if a resting state cannot be found for it. If a resting state cannot be found for the renewed position of a particle in Step 5.1 and Step 6, we simply set the fitness of the particle to be a number greater than the ever-achieved best value of itself.

V. TESTS AND RESULTS

The effectiveness of the proposed PPSO was verified by three identification tests as detailed below. In all the testing calculations, PPSO was empirically set with $n = 6$, $c_1 = c_2 = 1.4$,

TABLE V
SETTINGS OF PPSO FOR THE THREE METHODS OF TEST 1

	$l_{\max}$	$p_{\min,i}$	$p_{\max,i}$
Method (A1)	100	$0.7\bar{p}_i$	$1.3\bar{p}_i$
Method (A2)	500	$0.7\bar{p}_i$	$1.3\bar{p}_i$
Method (A3)	500	$0.5\bar{p}_i$	$1.5\bar{p}_i$

TABLE VI
DEVIATIONS AND RUNNING TIMES OF TEST 1 WITH METHOD (A1)

	scheme 1			scheme 2			scheme 3		
Run	E_V	E_C	time	E_V	E_C	time	E_V	E_C	time
1	1.3	14.9	4.1	1.7	11.3	3.1	1.5	12.2	6.3
2	0.9	8.0	5.0	2.3	13.1	3.4	1.3	9.6	6.6
3	1.1	15.8	4.5	1.2	8.4	3.0	1.7	12.7	6.7
4	1.6	5.3	4.1	1.3	16.0	3.3	0.9	12.0	7.4
5	1.5	9.1	4.0	2.4	9.7	3.3	3.0	14.7	4.7
6	0.8	8.5	3.9	1.2	10.4	3.4	1.4	6.4	7.3
7	2.4	10.4	3.8	1.8	15.0	3.0	0.8	6.4	6.0
8	1.1	12.1	4.2	2.1	8.8	3.2	2.2	8.4	5.1
9	1.1	8.4	4.2	2.7	14.7	3.3	2.2	7.9	5.7
10	1.2	13.0	4.3	1.9	10.4	3.1	2.2	7.0	5.4
mean	1.3	10.6	4.2	1.9	11.8	3.2	1.7	9.7	6.1

$q_{\max} = 4$, and $g_{\min} = 0.003$, and all the programs used were coded in MATLAB R2009 a (MathWorks, Inc., 2009) and ran on a computer of 2.10 GHz Intel core 2 Duo CPU T6570 and 2.00 GB RAM.

A. Test 1: Identifying the Default Parameters From Membrane Potential Data Using a Single Stimulus

Myocyte: the one represented by the BR equation with the default parameters listed in Table II.

Experimental data: $t_k, \bar{V}_{m,k}, \bar{i}_{\mathrm{Na},k}, \bar{i}_{s,k}, \bar{i}_{k1,k}, \bar{i}_{x1,k}$ and $[\bar{\mathrm{Ca}}^{2+}]_{i,k}$, for $k = 0, 1, \ldots, 5000$ with an equal time interval of 0.1 ms were produced by solving the BR equation using the method in Section II while a 40-μA/cm^2 current of 1-ms duration was applied at time = 50 ms. Note that $\bar{i}_{\mathrm{Na},k}, \bar{i}_{s,k}, \bar{i}_{k1,k}, \bar{i}_{x1,k}$ and $[\bar{\mathrm{Ca}}^{2+}]_{i,k}$ are the "experimentally measured" currents and calcium concentration, whereas $i_{\mathrm{Na}}, i_s, i_{k1}, i_{x1}$, and $[\mathrm{Ca}]_i$ denote those calculated by the BR equations to be regressed.

Method: Using each of the three grouping schemes, PPSO was run ten times independently with the settings in Table V, respectively.

Results: The results of this test with methods (A1), (A2), and (A3) are summarized, respectively, in Tables VI– VIII where E_V and E_C are normalized root-mean square error (NRMSE, %) for the potential and for the currents and calcium concentration defined as

$$E_V = \sqrt{K^{-1} \sum_{k=1}^{K} e_{V,k}^2} \tag{30}$$

$$E_C = \sqrt{K^{-1} \sum_{k=1}^{K} e_{C,k}^2} \tag{31}$$

where $e_{V,k}$ and $e_{C,k}$ are, respectively, the normalized absolute error (NAE, %) for the potential and for the currents and calcium concentration at time instant k and defined as

$$e_{V,k} = \left| \frac{\bar{V}_{m,k} - V_{m,k}}{\bar{V}_{\max} - \bar{V}_{\min}} \right| \times 100 \tag{32}$$

$$e_{C,k} = \frac{1}{5} \sum_{Y} \left| \frac{\bar{Y}_{m,k} - Y_{m,k}}{\bar{Y}_{\max} - \bar{Y}_{\min}} \right| \times 100 \tag{33}$$

with $Y = i_{\mathrm{Na}}, i_s, i_{k1}, i_{x1}$, and $[\mathrm{Ca}]_i$. The time for each run is in minutes, and the mean in the last row is a simple column average over the ten runs. Against the "experimental data." Figs. 1 –3 compare the potential, currents, and calcium concentration calculated using the parameters regressed in the best runs (in the sense of minimum E_V), respectively, with methods (A1), (A2), and (A3).

TABLE VII
DEVIATIONS AND RUNNING TIMES OF TEST 1 WITH METHOD (A2)

	scheme 1			scheme 2			scheme 3		
Run	E_V	E_C	time	E_V	E_C	time	E_V	E_C	Time
1	0.4	6.5	23.6	0.7	9.8	22.2	0.3	7.2	43.9
2	0.4	12.4	18.8	0.4	10.3	12.8	0.3	9.3	30.4
3	0.6	15.7	25.4	0.4	8.2	6.7	0.3	8.2	47.5
4	0.7	11.4	10.9	0.6	7.9	19.0	0.3	8.3	27.3
5	0.3	12.7	17.1	0.6	8.8	15.1	0.3	13.5	31.6
6	0.3	8.5	10.0	0.6	7.4	20.4	0.3	9.8	35.3
7	0.7	10.4	11.0	0.5	7.6	9.3	0.3	10.4	20.7
8	0.4	8.7	29.4	0.6	10.1	18.7	0.3	7.5	16.0
9	0.4	11.6	23.5	0.7	9.8	17.7	0.3	6.5	36.7
10	0.3	11.8	23.8	0.3	5.9	5.9	0.3	6.8	35.9
mean	0.4	11.0	19.4	0.5	8.6	14.8	0.3	8.7	32.5

TABLE VIII
DEVIATIONS AND RUNNING TIMES OF TEST 1 WITH METHOD (A3)

	scheme 1			scheme 2			scheme 3		
Run	E_V	E_C	time	E_V	E_C	time	E_V	E_C	Time
1	1.4	22.2	19.6	0.9	33.3	14.8	0.5	31.9	47.5
2	0.6	10.1	20.4	1.2	30.6	11.7	1.6	62.2	44.9
3	0.7	34.8	19.0	0.7	28.6	20.0	3.9	10.8	4.1
4	1.0	18.6	20.1	1.0	23.2	15.8	0.7	21.1	41.5
5	0.8	17.7	18.8	0.6	7.7	31.0	0.4	12.3	51.5
6	0.7	20.5	21.9	1.0	11.5	13.8	1.7	14.1	25.4
7	1.2	27.5	10.1	1.0	12.8	18.4	0.4	13.7	60.7
8	0.9	11.6	18.3	0.6	18.4	17.9	0.3	14.7	49.6
9	0.8	15.3	16.0	0.9	9.8	16.6	0.5	32.9	46.9
10	0.8	16.0	22.2	0.5	11.7	10.0	0.9	16.7	51.4
mean	0.9	19.4	18.6	0.8	18.8	17.0	1.1	23.0	42.4

Table IX collects the deviation information on the nine best runs obtained in this test with different grouping schemes and testing methods where the average relative deviation of parameters is defined as

$$D_P = \frac{1}{63} \sum_{i=1}^{63} \left| \frac{\bar{p}_i - p_i}{\bar{p}_i} \right| \times 100 \tag{34}$$

with p_i being the regressed value, and the maximum values for absolute E_V, E_C, and D_P are defined, respectively, as:

$$E_{V,\max} = \max\{e_{V,k}, k = 1, 2, \ldots, K\} \tag{35}$$

$$E_{C,\max} = \max\{e_{C,k}, k = 1, 2, \ldots, K\} \tag{36}$$

$$D_{P,\max} = \max\left\{ \left| \frac{\bar{p}_i - p_i}{\bar{p}_i} \right|, i = 1, 2, \ldots, 63 \right\} \times 100. \tag{37}$$

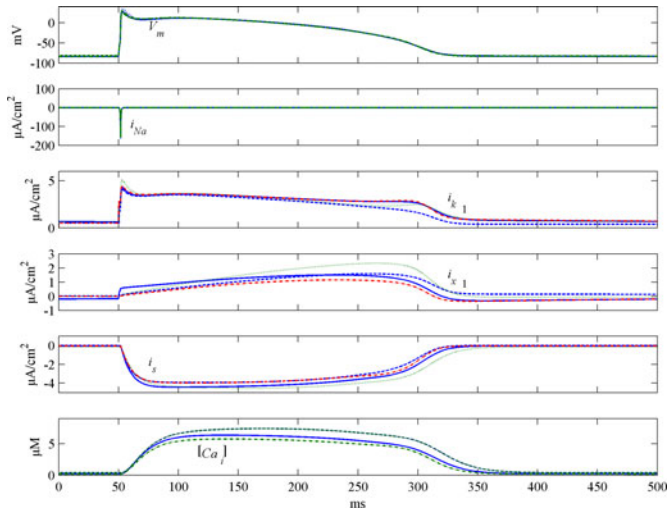

Fig. 1. Potential, currents, and Ca^{2+} concentration produced by the BR model using the default parameters (solid line) and those identified by PPSO in run 6 of scheme 1 (dash line), run 6 of scheme 2 (dot line), and run 7 of scheme 3 (dash-dot line) in test 1 with method (A1).

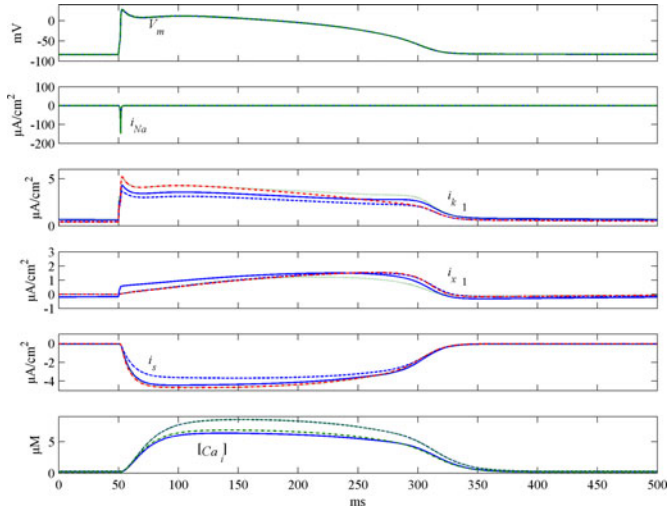

Fig. 2. Potential, currents, and Ca^{2+} concentration produced by the BR model using the default parameters (solid line) and those identified by PPSO in run 6 of scheme 1 (dash line), run 10 of scheme 2 (dot line), and run 9 of scheme 3 (dash-dot line) in test 1 with method (A2).

For comparison, this table also lists the results of Dokos and Lovell [8] using the same "experimental data" as those in this test and searching spaces of ± 10 and 30% around the default parameters, respectively, under entries DL-S10 and S30.

It is seen from Tables VI–VIII and Figs. 1–3 that in all the tests with different grouping schemes and searching spaces, PPSO well fit the potential (mean E_V: 0.3–1.9%), but produced quite large prediction errors for the four currents and Ca^{2+} concentration (mean E_C: 8.6–23.0%). With the "experimental data" from a single stimulus, the fits obtained with PPSO are comparable with those reported by Dokos and Lovell [8] as shown in Table IX. At this point, it should be noted that as demonstrated by Dokos and Lovell, identifying the BR equation parameters is a problem without local identifiability: the "correct" parameters cannot be recovered from only membrane potential data under

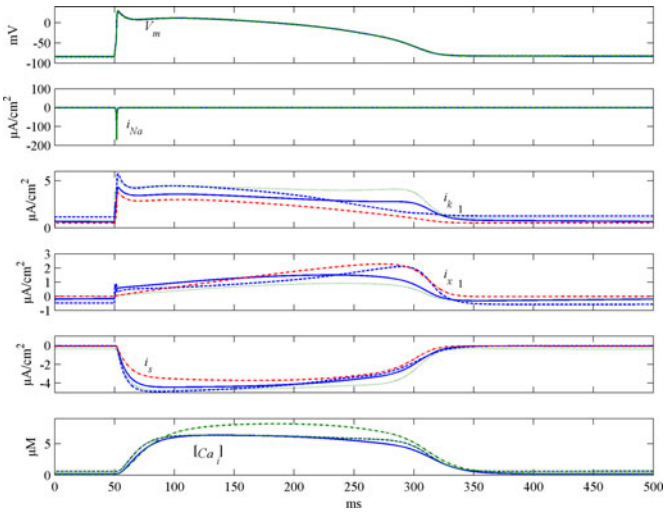

Fig. 3. Potential, currents, and Ca^{2+} concentration produced by the BR model using the default parameters (solid line) and those identified by PPSO in run 2 of scheme 1 (dash line), run 10 of scheme 2 (dot line), and run 8 of scheme 3 (dash-dot line) in test 1 with method (A3).

TABLE IX
DEVIATIONS FOR THE NINE BEST SOLUTIONS OF TEST 1

Method	Run	E_V	E_C	D_P	$E_{V,\max}$	$E_{C,\max}$	$D_{P,\max}$
(A1)	6[a]	0.8	8.5	8.9	4.8	28.0	30.0
	6[b]	1.2	10.4	12.6	0.9	37.9	30.0
	7[c]	0.8	6.4	7.9	4.9	36.2	27.8
(A2)	6[a]	0.3	8.5	11.5	1.4	44.3	30.0
	10[b]	0.3	5.9	9.7	1.1	41.4	29.3
	9[c]	0.3	6.5	9.6	3.1	43.7	30.0
(A3)	2[a]	0.6	10.1	22.4	3.4	36.9	50.0
	10[b]	0.5	11.7	17.8	3.7	33.4	47.6
	8[c]	0.3	14.7	16	3.8	55.9	45.5
DL-S10		0.6	15.2	14.5	0.5	67.1	41.3
DL-S30		0.5	10.7	8.5	1.0	45.2	45.2

Note: a, b and c mean that schemes 1, 2 and 3 were used, respectively.

a single stimulus, and multiple distinct parameter sets can fit the data equally well. Membrane potential data from complex stimuli are needed in order to reconstruct the underlying membrane currents and cytosolic calcium concentration.

Tables VI–VIII also indicate that on average, the fitting errors (E_V's and E_C's) are comparable for the models identified by PPSO using different grouping schemes, and the running time of PPSO increases with the increase of the number of parameter groups included in the grouping schemes. Though the performance of PPSO was not apparently influenced by the grouping scheme, parameter grouping did help much in the searching process as illustrated in Fig. 4, which depicts the fitness of the best particle and the number of consecutive generations of non-improvement q for run 6 of scheme 1 using method (A1). As shown in this figure, the strategy of partial perturbation was applied in, among others, generations 15, 27, 35 and so on, where $q > 4$. In generations 35, 42, and 75, partial perturbation initiated significant decreases in the fitness of the best particle.

Furthermore, the results in Table VIII indicate that PPSO performed quite well even in a searching space of $\pm 50\%$ around the default parameters of the BR equation. Because of its inherent

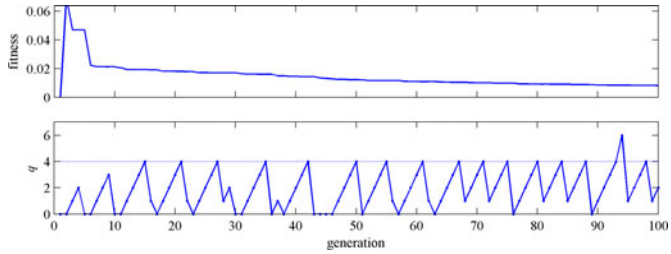

Fig. 4. Fitness and number of consecutive generations of nonimprovement (q) in the evolution of PPSO in run 6 of scheme 1, test 1 with method (A1).

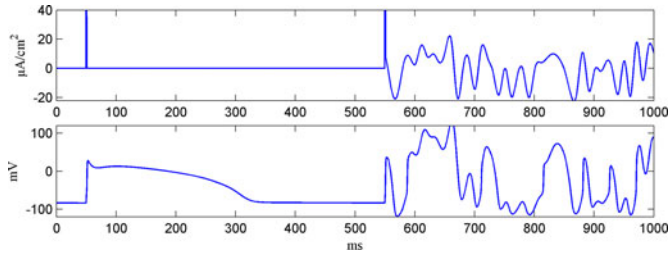

Fig. 5. Stimulating current (top panel) and membrane potential (bottom panel) generated with $N(\mu = 0, \sigma = 20)$ μA/cm^2.

TABLE X
NUMBER OF EFFECTIVE APPLICATIONS OF THE PARAMETER PATTERNS

pattern	Run										mean
	1	2	3	4	5	6	7	8	9	10	
1	2	0	3	1	0	1	2	1	3	3	1.6
2	0	1	1	2	2	0	1	0	0	0	0.7
3	0	3	1	1	1	1	1	1	0	0	0.9
4	1	0	1	0	1	1	0	0	0	0	0.4
5	1	0	0	0	1	3	0	2	2	1	1
6	1	2	2	1	2	1	0	2	1	2	1.4
7	2	1	1	2	0	1	1	2	1	0	1.1
8	1	0	0	0	0	2	0	0	0	1	0.4
9	4	2	0	2	1	0	0	0	0	1	1
10	1	1	0	1	2	2	3	1	2	1	1.4
11	1	1	2	1	1	2	3	2	2	1	1.6
12	0	2	0	0	0	0	0	1	0	0	0.3
13	0	1	1	3	0	0	1	0	1	0	0.7
14	0	0	3	1	1	0	0	0	0	0	0.5
15	1	4	4	0	2	2	0	2	0	3	1.8

randomness, PPSO is insensitive to initial values and suitable for large searching spaces.

At the end of this section, Table X lists the number of effective applications of the 15 parameter patterns of scheme 1 in test 1 with method (A1), where an effective application means a decrease of the fitness caused by partially perturbing the parameters according to a pattern as implemented in Step 5 of the PPSO algorithm. It is seen from this table that every pattern had its opportunity to make some contribution.

B. Test 2: Identifying the Default Parameters From a Single Action Potential and Randomly Perturbed Waveform

Myocyte: the same as the one in Test 1.

Experimental data: t_k, $\bar{V}_{m,k}, \bar{i}_{\mathrm{Na},k}, \bar{i}_{s,k}, \bar{i}_{k1,k}, \bar{i}_{x1,k}$, and $[\bar{\mathrm{Ca}}^{2+}]_{i,k}$, for $k = 0, 1, \ldots, 10^4$ with an equal time interval of 0.1 ms were produced by solving the BR equation using the method in Section II while a 40-μA/cm^2 current pulse with 1-ms duration was applied, respectively, at time = 50 and 550 ms, and a pseudorandom current was continuously injected after 550.1 ms. As shown in Fig. 5, the pseudorandom current comprised of cubic spline segments whose magnitudes followed a normal distribution $N(\mu = 0, \sigma = 20)$ μA/cm^2 at instants every 8.3 ms after time = 550 ms.

Method: Using each of the three grouping schemes, PPSO was run ten times independently with $l_{\max} = 500$, and $p_{\min,i} = 0.9\bar{p}_i$ and $p_{\max,i} = 1.1\,\bar{p}_i$ for $i = 1, 2, \ldots, 63$. Thirty sets of parameters were thus regressed and used to reproduce the "experimental"

TABLE XI
DEVIATIONS AND RUNNING TIMES OF TEST 2

	scheme 1			scheme 2			scheme 3		
Run	E_V	E_C	time	E_V	E_C	time	E_V	E_C	time
1	0.6	2.2	140.5	1.1	2.3	58.3	0.7	2.2	117.5
2	1.6	2.8	123.7	1.4	2.5	56.9	0.5	5.6	82.8
3	0.8	2.2	118.1	0.7	2.0	44.0	1.7	5.9	106.2
4	0.5	2.6	139.1	1.2	2.8	62.1	0.6	4.7	108.4
5	1.0	2.5	131.4	1.8	6.2	62.1	0.5	3.9	112.1
6	0.4	2.7	141.8	1.1	2.6	64.4	1.0	2.4	110.9
7	0.9	3.3	119.8	0.9	3.0	68.9	0.8	3.3	114.1
8	1.5	4.9	130.7	1.2	4.6	61.7	0.7	1.7	113.5
9	1.2	2.0	116.9	0.5	3.6	63.3	1.0	6.0	127.1
10	1.4	7.6	123.0	2.7	6.7	64.6	0.7	5.9	115.7
mean	1.0	3.3	128.5	1.3	3.6	60.6	0.8	4.2	110.8

TABLE XII
MAXIMUM OF THE NAE FOR THE POTENTIAL AND FOR THE CURRENTS AND CALCIUM CONCENTRATION IN TEST 2

	Scheme 1		Scheme 2		Scheme 3	
Run	$E_{V,\max}$	$E_{C,\max}$	$E_{V,\max}$	$E_{C,\max}$	$E_{V,\max}$	$E_{C,\max}$
1	4.3	4.5	4.0	5.5	3.1	3.8
2	4.3	6.9	3.7	5.1	1.5	8.4
3	1.7	3.2	2.9	3.8	13.4	12.7
4	2.1	3.8	10.3	8.6	4.2	7.7
5	2.9	4.4	6.1	5.4	5.0	6.0
6	1.7	4.1	12.5	7.4	3.1	3.7
7	3.8	5.0	4.1	4.0	4.5	5.5
8	4.8	8.5	3.3	7.4	6.7	6.0
9	2.7	3.1	14.6	10.3	4.8	11.0
10	8.5	10.4	16.9	14.4	13.1	12.2

potential, current, and calcium concentration data caused by the first current pulse (in the time interval 0–500 ms).

Results: Table XI lists the NRMSE for the potential (E_V) and the currents and calcium concentration (E_C) as defined in (30) and (31), respectively. Comparison between the data in this table with those in Tables VI–VIII shows that the four currents and the calcium concentration were predicted much more accurately in this test (the 30-run average of E_C's is 3.7) than in Test 1 where the 30-run average of E_C's is 11.2, 9.4, and 20.4 for methods (A1), (A2), and (A3), respectively, which justifies the suggestion of Dokos and Lovell [8] that membrane potential data from complex stimuli are necessary for reconstructing the underlying membrane currents and cytosolic calcium concentration.

The data in Table XI also indicate that the NRMSE for the potential (E_V) is not a good indicator for the prediction error of the currents and calcium concentration (E_C). In order to find such an indicator, Table XII lists the maximum values for the NAE of the potential and of the currents and calcium concentration, as defined in (35) and (36). It was observed that the

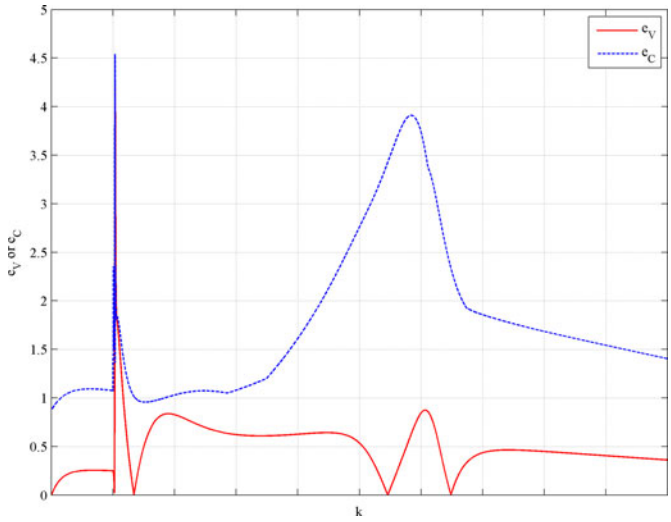

Fig. 6. e_V and e_C for run 1 of scheme 1 in test 2 ($\sigma = 20\ \mu$A/cm^2).

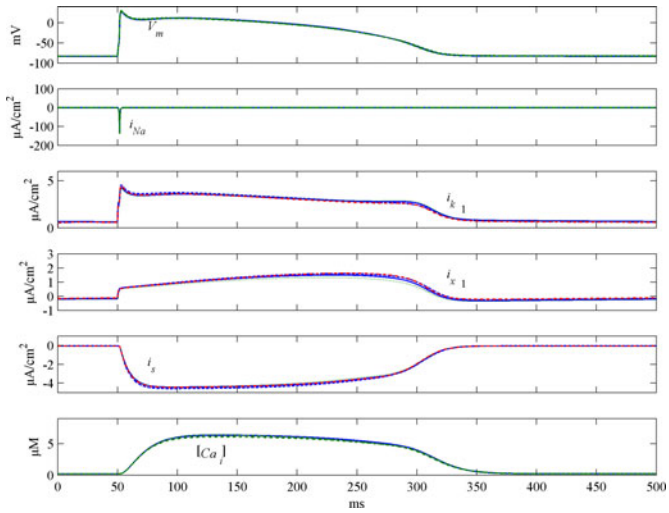

Fig. 7. Potential, currents, and Ca^{2+} concentration produced by the BR model using the default parameters (solid line) and those identified by PPSO in run 3 of scheme 1 (dash line), run 3 of scheme 2 (dot line), and run 1 of scheme 3 (dash-dot line) in test 2 ($\sigma = 20\ \mu$A/cm^2).

error curves $e_{V,k}$ and $e_{C,k}$ as defined in (32) and (33), versus $k, k = 1, 2, \ldots, K$, as illustrated in Fig. 6, are quite complex and vary drastically from run to run. However, as a qualified fit, the maximum error $(E_{V,\max})$ of fitting for the potential should not exceed some upper threshold $(UE_{V,\max})$, that is, $E_{V,\max} < UE_{V,\max}$. At the same, we also observed from the error curves that too small $E_{V,\max}$ usually means great E_C, though the potential is accurately fitted. To have a reasonable prediction for the four currents and the calcium concentration with parameters regressed from potential data only, we also need to control $E_{V,\max}$ not to be smaller than some lower threshold $(LE_{V,\max})$, that is, $E_{V,\max} > LE_{V,\max}$. For practical application of the BR model, we set empirically $UE_{V,\max} = 3-3.1$ and $LE_{V,\max} = 1.7-2$ from observing the error curves. With these lower and upper thresholds, eight sets of parameters for the BR equation are picked out as highlighted in Tables XI and XII, which are expected to reconstruct well the potential, currents, and calcium concentration simultaneously.

Among the ten runs with scheme 1, there are five sets of parameters which can well reconstruct the four currents and calcium concentration. At this point, we may say that scheme 1 is probably more suitable for grouping the parameters than schemes 2 and 3, since overly simple (scheme 2) or overly subtle (scheme 3) grouping of the BR equation parameters may produce distorted parameters that fit the potential data precisely, but fail to predict the currents and calcium concentration well. In addition, scheme 1 may profit from its grouping method where the constituting features of the BR model are considered.

In Fig. 7, curves are depicted for the potential, currents, and calcium concentration calculated, respectively, with three sets of parameters regressed with different grouping schemes. It is seen from this figure that the underlying membrane currents and cytosolic calcium concentration were well reconstructed. The errors corresponding to Fig. 7 are listed in Table XIII in contrast to those (DL-R10) associated with the parameters regressed by Dokos and Lovell [8] from a single action potential and

TABLE XIII
DEVIATIONS WITH THE THREE SETS OF PARAMETERS OF TEST 2

Scheme	Run	E_V	E_C	D_P	$E_{V,\max}$	$E_{C,\max}$	$D_{P,\max}$
1	3	0.8	2.2	2.4	0.7	7.1	7.7
2	3	0.7	2.0	3.0	2.9	11.5	9.1
3	1	0.7	2.2	2.9	1.1	8.6	9.8
DL-R10		0.9	1.8	10.4	2.5	5.1	35.6

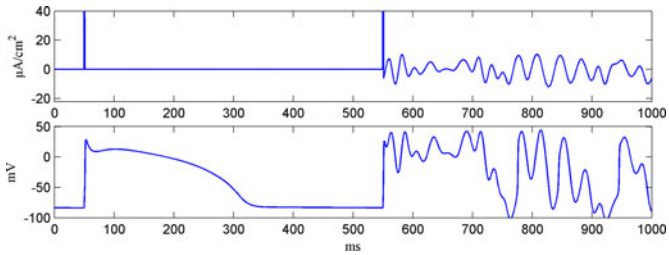

Fig. 8. Stimulating current (top panel) and membrane potential (bottom panel) generated with $N(\mu = 0, \sigma = 10)\ \mu$A/cm^2.

perturbed waveform generated using a mean hyperpolarising injected current of 10 μA/cm^2.

Grouping scheme 1 was further tested using another two sets of experimental data generated the same way as stated at the beginning of this section except for $\sigma = 10$ and 15 μA/cm^2, respectively. The experimental data for $\sigma = 10\ \mu$A/cm^2 are shown in Fig. 8. The same test method as stated at the beginning of this section was adopted except that only five independent runs were conducted. The results of these two additional tests are summarized in Table XIV. Applying criterion $LE_{V,\max} < E_{V,\max} < UE_{V,\max}$, we picked out three sets of parameters as highlighted in Table XIV, which well reconstruct the potential, currents, and calcium concentration as shown in Fig. 9.

At this point, it is noted that design of the stimulating current is a meaningful problem of constrained optimization where the current should be electrophysiologically practical, easy to be experimentally implemented, and able to excite as many

TABLE XIV
RESULTS OF TESTS WITH SCHEME 1 AND USING RANDOMLY PERTURBED WAVEFORMS OF $\sigma = 10$ AND 15 μA/CM^2

	$\sigma = 10$				$\sigma = 15$			
Run	E_V	E_C	$E_{V,\max}$	$E_{C,\max}$	E_V	E_C	$E_{V,\max}$	$E_{C,\max}$
S1	0.5	4.8	11.2	8.2	0.8	3.9	12.0	8.4
S2	0.5	2.2	2.9	3.6	0.6	2.7	2.4	4.2
S3	0.7	3.7	4.9	5.5	1.6	6.4	17.8	16.1
S4	0.5	2.8	6.3	6.1	1.0	2.6	11.2	8.9
S5	1.2	4.2	29.3	19.6	0.9	3.8	2.0	6.1
mean	0.7	3.5			0.8	3.2		

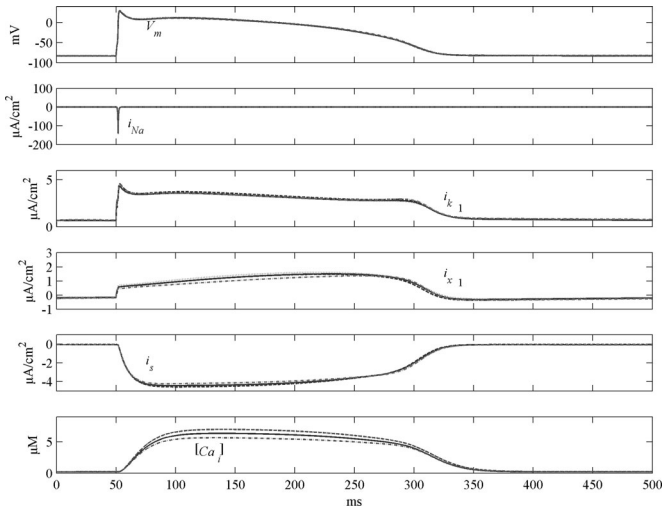

Fig. 9. Potential, currents, and Ca^{2+} concentration produced by the BR model using the default parameters and (solid line) and those identified by PPSO in run S2 of $\sigma = 10$ μA/cm^2 (dash line), run S2 of $\sigma = 15$ μA/cm^2 (dot line), and run S5 of $\sigma = 15$ μA/cm^2 (dash-dot line) in test 2.

as detailed features of the model in the responding potential waveform. The randomly perturbed waveforms as suggested by Dokos and Lovell [8] were used mainly to demonstrate the capability of PPSO in identifying the BR equations, while other better forms for stimulating currents are left to be studied.

C. Test 3: Identifying the BR Equation Parameters From Potential Data of a Single Stimulus Generated by Luo and Rudy (LR) Model

Myocyte: the one described by the LR model [14]. The LR model includes six ionic currents: fast sodium current $I_{\rm Na}$, slow inward current I_{si}, time-dependent potassium current I_K, time-independent potassium current I_{K1}, plateau potassium current I_{Kp}, and background current I_b. The first two $(I_{\rm Na}, I_{si})$ are inward currents, whereas the left four are outward currents. A rough equivalence can be made between these six currents and the four currents of the BR model: $i_{\rm Na} = I_{\rm Na}, i_s = I_{si}, i_{x1} = I_K, i_{k1} = I_{K1} + I_{Kp} + I_b$.

Experimental data: t_k, $\bar{i}_{{\rm Na},k} = \bar{I}_{{\rm Na},k}, \bar{i}_{s,k} = \bar{I}_{{\rm si},k}, \bar{i}_{x1,k} = \bar{I}_{K,k}, \bar{i}_{k1,k} = \bar{I}_{K1,k} + \bar{I}_{{\rm Kp},k} + \bar{I}_{b,k}, \bar{V}_{m,k}$, and $[\bar{\rm Ca}^{2+}]_{i,k}$ for $k = 0, 1, \ldots, 5000$ with an equal time interval of 0.1 ms were produced by solving the LR model while a 40-μA/cm^2 current with a 1-ms duration was applied at time = 50 ms. The method for solving the LR model was the same as that stated in Section II, except that the equations for the BR model were replaced by the LR equations. Note that $\bar{I}_{\rm Na}, \bar{I}_{\rm si}, \bar{I}_K, \bar{I}_{K1}, \bar{I}_{\rm Kp}, \bar{I}_b, \bar{V}_m$, and $[\bar{\rm Ca}^{2+}]_{i,k}$ are the "experimentally measured" currents, potential, and calcium concentration.

TABLE XV
DEVIATIONS AND RUNNING TIMES OF TEST 3

	scheme 1			scheme 2			scheme 3		
Run	E_V	E_C	time	E_V	E_C	time	E_V	E_C	time
1	1.0	20.1	20.2	1.0	19.5	16.4	1.0	16.6	36.8
2	0.9	19.6	21.5	1.2	18.3	16.3	0.9	19.5	45.2
3	0.9	18.6	23.4	2.7	17.7	15.2	1.0	25.1	43.7
4	1.1	25.0	21.7	1.2	21.7	17.6	0.7	21.9	42.4
5	0.8	20.6	22.9	1.3	25.2	15.8	0.7	20.7	47.3
6	0.9	21.2	20.1	1.0	19.4	16.8	0.6	20.9	43.7
7	1.1	16.3	19.9	1.3	20.5	13.7	0.7	22.9	45.9
8	0.8	22.3	21.8	1.9	20.5	15.8	1.8	23.4	35.0
9	1.1	23.2	13.9	1.7	19.0	16.5	0.7	22.9	46.1
10	1.2	16.5	18.9	2.2	24.7	15.4	1.2	27.0	44.6
mean	1.0	20.3	20.4	1.5	20.7	15.9	0.9	22.1	43.1

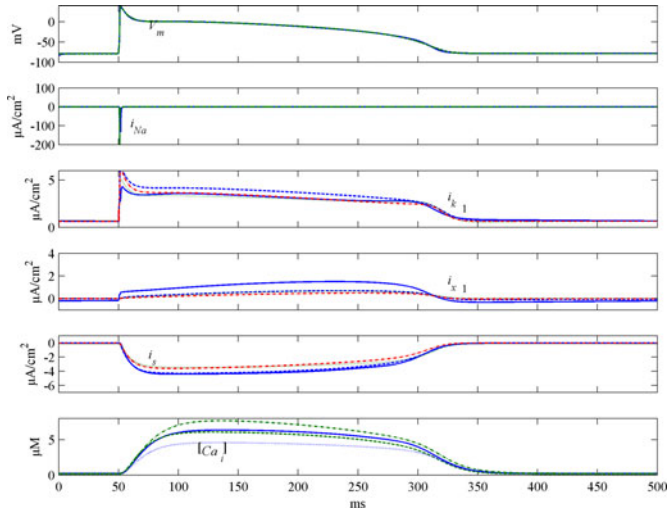

Fig. 10. Potential, currents, and Ca^{2+} concentration produced by the LR model (experimental data, solid line) and by the BR model using the parameters identified by PPSO in run 8 of scheme 1 (dash line), run 1 of scheme 2 (dot line), and run 6 of scheme 3 (dash-dot line) in test 3.

Method: With each of the three grouping schemes, PPSO was run ten times independently with $l_{\max} = 500$, and $p_{\min,i} = 0.7\bar{p}_i$, and $p_{\max,i} = 1.3\bar{p}_i$ for $i = 1, 2, \ldots, 63$.

Results: The deviations and running times as defined in test 1 are listed in Table XV for this test. Fig. 10 compares the potential, currents, and calcium concentration calculated using the best sets of parameters regressed with the three grouping schemes (in the sense of minimum E_V). It is seen from this table and this figure that as expected, the potential is fitted accurately, however, the underlying currents and calcium concentration are predicted with gross error. The NRMSE for the currents and calcium concentration E_C is about 20% in this test, nearly double of that in Table VII of test 1, which may be attributed to the roughness of the above equivalence between the ionic currents of the LR model and those of the BR equations.

VI. CONCLUSION AND DISCUSSION

1) A partially perturbed PSO (PPSO) has been proposed for identifying the parameters of the BR equation from

membrane potential data for a myocyte. As shown by the results of tests 1 and 3 where single action potential data were used, PPSO is efficient for different myocytes in the sense that it can minimize the fitting error of the action potential within reasonable time and with initial values randomly selected in spaces as large as $\pm 30\%$ or $\pm 50\%$ of the default values.

2) The results of test 2 show that scheme 1 is probably more suitable for grouping the parameters than schemes 2 and 3. With scheme 1, PPSO can effectively identify the BR equation parameters from a single action potential and randomly perturbed stimulus waveform. The underlying membrane currents and cytosolic calcium concentration can be well reconstructed with parameters identified this way.

In discussion, two points are presented as follows.

1) PPSO is specific to the identification of the BR equation parameters, but the idea for its design may be useful in estimating the parameters of other Hodgkin–Huxley type models. The algorithm parameters for PPSO, such as the number of particles, maximum number of generations, etc., were set empirically with much arbitrariness.
2) A large searching space surely reduces the efficiency of PPSO or any other minimization algorithm. When the parameters vary in a large space, PPSO will frequently run to particles for which the coordinates are simply unacceptable as a set of parameters for the BR equation. As a matter of fact, methods for setting initial values and searching space reasonable for a given problem are themselves valuable.

ACKNOWLEDGMENT

The authors are grateful to T. Guo, Graduate School of Biomedical Engineering, University of New South Wales, Sydney, N.S.W., Australia, for his constructive discussion, and thank the reviewers for their comments that help to improve the manuscript greatly.

REFERENCES

[1] A. L. Hodgkin and A. F. Huxley, "A quantitative description of membrane current and its application to conduction and excitation in nerve," *J. Physiol.*, vol. 117, pp. 500–544, Aug. 1952.
[2] D. Noble, "A modification of the Hodgkin–Huxley equations applicable to Purkinje fibre action and pace-maker potentials," *J. Physiol.*, vol. 160, no. 2, pp. 317–352, Feb. 1962.
[3] R. E. McAllister, D. Noble, and R. W. Tsien, "Reconstruction of the electrical activity of cardiac Purkinje fibres," *J. Physiol.*, vol. 251, no. 1, pp. 1–59, Sep. 1975.
[4] G. W. Beeler and H. Reuter, "Reconstruction of the action potential of ventricular myocardial fibres," *J. Physiol.*, vol. 268, pp. 177–210, Jun. 1977.
[5] J. P. Drouhard and F. A. Roberge, "The simulation of repolarization events of the cardiac Purkinje fiber action potential," *IEEE Trans. Biomed. Eng..*, vol. BME-29, no. 7, pp. 481–493, Jul. 1982.
[6] J. P. Drouhard and F. A. Roberge, "A simulation study of the ventricular myocardial action potential," *IEEE Trans. Biomed. Eng.*, vol. BME-29, no. 7, pp. 494–502, Jul. 1982.
[7] D. DiFrancesco and D. Noble, "A model of cardiac electrical activity incorporating ionic pumps and concentration changes," *Phil. Trans. R. Soc. B.*, vol. 307, pp. 353–398, Jan. 1985.
[8] S. Dokos and N. H. Lovell, "Parameter estimation in cardiac ionic models," *Prog. Biophys. Mol. Biol.*, vol. 85, pp. 407–431, Jun./Jul. 2004.
[9] Z. Syed, E. Vigmond, S. Nattel, and L. J. Leon, "Atrial cell action potential parameter fitting using genetic algorithms," *Med. Biol. Eng. Comput.*, vol. 43, pp. 561–571, Sep. 2005.
[10] F. Liu, J. Walmsley, and K. Burrage (2010, Nov.). "Parameter estimation for a phenomenological model of the cardiac action potential," Presented at The 15th Biennial Computational Techniques and Applications Conf. [Online]. Available: http://conferences.science.unsw.edu.au/CTAC2010/FawangLiuCTAC10.pdf
[11] N. Mathavan, "Parameter optimization in simplified models of Cardiac Myocytes," M.S. thesis, Dept. Biol. Eng., UNSA Sydney SA, Australia, 2009
[12] J. Kennedy and R. C. Eberhart, "Particle swarm optimization," in *Proc. 4th IEEE Int. Conf. Neural Netw.*, Perth, Australia, 1995, pp. 1942–1948.
[13] Z. Yang, J. Fang, J. Li, and S. Zeng, "Application of particle swarm optimization to multiparameters fitting," *J. Zhejiang Normal Univ. (Nat. Sci.)*, vol. 31, no. 2, pp. 173–177, 2008.
[14] C. H. Luo and Y. Rudy, "A model of the ventricular cardiac action potential. Depolarization, repolarization, and their interaction," *Circulation Res.*, vol. 68, no. 6, pp. 1501–1526, Jun. 1991.

Authors' photographs and biographies not available at the time of publication.